

SPE 59314

## Relative Permeability Correlation for Mixed-Wet Reservoirs

A. Kjosavik, J.K. Ringen, Statoil, S.M. Skjæveland, Stavanger College

Copyright 2000, Society of Petroleum Engineers Inc.

This paper was prepared for presentation at the 2000 SPE/DOE Improved Oil Recovery Symposium held in Tulsa, Oklahoma, 3–5 April 2000.

This paper was selected for presentation by an SPE Program Committee following review of information contained in an abstract submitted by the author(s). Contents of the paper, as presented, have not been reviewed by the Society of Petroleum Engineers and are subject to correction by the author(s). The material, as presented, does not necessarily reflect any position of the Society of Petroleum Engineers, its officers, or members. Papers presented at SPE meetings are subject to publication review by Editorial Committees of the Society of Petroleum Engineers. Electronic reproduction, distribution, or storage of any part of this paper for commercial purposes without the written consent of the Society of Petroleum Engineers is prohibited. Permission to reproduce in print is restricted to an abstract of not more than 300 words; illustrations may not be copied. The abstract must contain conspicuous acknowledgment of where and by whom the paper was presented. Write Librarian, SPE, P.O. Box 833836, Richardson, TX 75083-3836, U.S.A., fax 01-972-952-9435.

### Abstract

A two-phase (oil-water) relative permeability correlation for mixed-wet reservoir rock is developed and validated in this paper, including bounding drainage and imbibition processes and scanning hysteresis loops, all integrated with the corresponding changes in capillary pressure.

The Corey-Burdine type relative permeability correlation is widely used in the industry. It was originally developed for water-wet reservoirs from a Brooks-Corey power-law capillary pressure correlation in combination with a bundle-of-tubes model of the pore network.

We have adjusted the Brooks-Corey capillary pressure correlation to be valid for mixed-wet rock and now present the ensuing Corey-Burdine relative permeability correlation for mixed-wet reservoirs.

The functional form of the relative permeability correlation is symmetric with respect to fluid-dependent properties since neither fluid is privileged in a mixed-wet environment. It reverts to the standard Corey-Burdine correlation for the completely water- or oil-wet case. A water-wet behavior is displayed at low water saturations and an oil-wet behavior at low oil saturations, in accordance with experiments. The correlation provides an inverted S-shape oil relative permeability curve with an inflection point, and closed hysteresis scanning loops, as observed.

The correlation is validated by comparison with measured relative permeability curves and simultaneously measured capillary pressure and relative permeability curves from the literature.

The correlations and hysteresis logic are easily programmed, and we suggest that the Killough hysteresis model, employed in many numerical reservoir simulators, should be updated with the new scheme.

### Introduction

In an earlier paper<sup>1</sup>, we presented a capillary pressure correlation for mixed-wet reservoirs and suggested to extend the Corey-Burdine<sup>2,3</sup> relative permeability relationships from water-wet to mixed-wet conditions. In the present paper, we develop this idea further and include hysteresis logic, integrated with the capillary pressure hysteresis loops.

The main design constraints of the relative permeability correlation are

1. the functional form is symmetric with respect to the two fluids oil and water. That is, the functional form is invariant to interchange of index  $o$  with index  $w$ .
2. the hysteresis loops are closed,<sup>4</sup>
3. the hysteresis loops of the capillary pressure and the relative permeabilities form a consistent set,<sup>5,6</sup>
4. imbibition oil relative permeability curves have the characteristic inverted 'S' shape.<sup>7-13</sup>

The validity of the relative permeability correlation and the integrated hysteresis schemes are verified by detailed, published relative permeability measurements<sup>4</sup> and by simultaneously measured hysteretic relative permeability and capillary pressure curves.<sup>5</sup>

The integrated hysteresis scheme is easily programmable and could replace the Killough-scheme<sup>14</sup> which presently is the most common in use in numerical reservoir simulators.

There is now wide acceptance of the view that most reservoirs are at wettability conditions other than water-wet, and network-models<sup>15</sup> incorporate this fact. However, to incorporate mixed-wet rock properties into a numerical reservoir simulator, validated correlations are required.<sup>16-18</sup>

### Review of Capillary Pressure Correlation

The relative permeability correlation is derived from the capillary pressure correlation<sup>1</sup> and a review is given here. A sketch of the capillary pressure curve correlation for mixed-wet rock is shown in **Fig. 1**. It is an extension of the Brooks and Corey<sup>19,20</sup> correlation for primary drainage of a completely water-wet reservoir, which may be written as

$$p_{cd} = \frac{c_{wd}}{\left(\frac{S_w - S_{wr}}{1 - S_{wr}}\right)^{a_{wd}}}, \dots\dots\dots (1)$$

where  $c_{wd}$  is the entry pressure,  $1/a_{wd}$  the pore size distribution index,<sup>2</sup> and  $S_{wr}$  is residual (or irreducible) water saturation.

For primary imbibition of a completely oil-wet rock, i.e., reduction of oil saturation from  $S_o = 1$ , the capillary pressure is also represented by Eq. 1, with index  $w$  replaced by  $o$ .

For the intermediate cases, the capillary pressure correlation is the sum of the two extremes,

$$p_c = \frac{c_w}{\left(\frac{S_w - S_{wr}}{1 - S_{wr}}\right)^{a_w}} + \frac{c_o}{\left(\frac{S_o - S_{or}}{1 - S_{or}}\right)^{a_o}}, \dots\dots\dots (2)$$

where the  $a_w$ ,  $a_o$  and  $c_w$  are constant, positive numbers, while the  $c_o$  is constant and negative. There is one set of constants for imbibition and another for drainage. The first term of Eq. 2 is the ‘water branch’, the second the ‘oil branch’. Also, we use the term ‘drainage’ if  $S_w$  is decreasing, and ‘imbibition’ if  $S_w$  is increasing, irrespective of the wettability preference.

**Hysteresis Loop Logic.** The design constraints follow from experimental evidence:<sup>21-26</sup>

1. A saturation reversal on the primary drainage curve, before reaching the residual water saturation  $S_{wr}$ , **Fig. 2**, spawns an imbibition scanning curve aiming at a residual oil saturation determined by Land’s trapping relation.
2. Reversal from the primary drainage curve at  $S_{wr}$  starts an imbibition scanning curve down to  $S_{or}$ . This curve is labeled (b) in **Fig. 1**, and is the bounding imbibition curve.
3. The secondary drainage curve, labeled (c) in **Fig. 1**, is defined by a reversal from the bounding imbibition curve at  $S_{or}$ . Together, the bounding imbibition and the secondary (bounding) drainage curves constitute the closed bounding hysteresis loop.
4. All drainage scanning curves that emerge from the bounding imbibition curve, scan back to  $S_{wr}$ , **Fig. 3**, and all reversals from the bounding drainage curve scan to  $S_{or}$ , **Fig. 4**.
5. A scanning curve originating from  $S_w[k]$ , the  $k$ ’th reversal saturation, will trace back to  $S_w[k-1]$  and form a closed scanning loop, unless a new reversal occurs.
6. If a scanning curve tracing back from  $S_w[k]$  reaches  $S_w[k-1]$  before any new reversal, i.e., forms a closed scanning loop, the process continues by retracing the path of the  $[k-2]$  reversal as if the  $[k-1]$  reversal had not occurred, as shown in **Fig. 5**.
7. The shape of a scanning loop is similar to the bounding loop since the  $a$  and  $c$  parameters are constants for a given rock-fluid system.

All properties of the  $k$ ’th scanning curve are labeled by  $[k]$ . The capillary pressure is denoted by  $p_{ca}[k]$ , where  $a$  is either  $i$  for imbibition or  $d$  for drainage. By convention,  $k$  is an odd number for imbibition and even number for drainage, 0 denoting the primary drainage process. The asymptotes of the scanning curves are denoted by  $S_{wr}[k]$  and  $S_{or}[k]$ , and the (water) reversal saturation is denoted by  $S_w[k]$ . The fixed, ‘global’ residual saturations of the bounding hysteresis loop are denoted by  $S_{wr}$  and  $S_{or}$ .

All scanning curves are modeled by the same constants  $a$  and  $c$  as the bounding curves. As an example of the notation, the primary drainage capillary pressure is denoted by  $p_{cd}[0]$ , and its value at the first reversal,  $S_w[1]$ , is given by  $p_{cd}[0](S_w[1])$ .

**First Reversal.** A reversal from primary drainage results in an imbibition scanning curve  $p_{ci}[1]$ , scanning towards  $S_{or}[1]$ . At the point of saturation reversal,  $S_w[1]$ , the imbibition scanning curve is equal to the primary drainage curve,

$$p_{ci}[1](S_w[1]) = p_{cd}[0](S_w[1]), \dots\dots\dots (3)$$

where  $p_{cd}[0](S_w[1])$  is given by

$$p_{cd}[0](S_w[1]) = \frac{c_{wd}}{\left(\frac{S_w[1] - S_{wr}}{1 - S_{wr}}\right)^{a_{wd}}}, \dots\dots\dots (4)$$

and  $p_{ci}[1](S_w[1])$  by

$$p_{ci}[1](S_w[1]) = \frac{c_{wi}}{\left(\frac{S_w[1] - S_{wr}[1]}{1 - S_{wr}[1]}\right)^{a_{wi}}} + \frac{c_{oi}}{\left(\frac{S_o[1] - S_{or}[1]}{1 - S_{or}[1]}\right)^{a_{oi}}}. \dots\dots\dots (5)$$

To satisfy Eq. 3, we adjust the ‘water asymptote’  $S_{wr}[1]$ , and let the scanning curve aim at the ‘oil asymptote’  $S_{or}[1]$ , determined by Land’s equation,

$$\frac{1}{S_{or}[1]} - \frac{1}{S_o[1]} = C, \dots\dots\dots (6)$$

where  $C$  is Land’s trapping constant for the porous medium, and  $S_o[1] = 1 - S_w[1]$ . In the limit, when the reversal from the primary drainage curve starts at  $S_w[1] = S_{wr}$ , the imbibition scanning curve becomes identical to the bounding imbibition curve. **Fig. 2** shows scanning curves originating from two different values of  $S_w[1]$ , as well as the bounding hysteresis loop where  $S_w[1] = S_{wr}$ .

**Second Reversal.** A reversal on the scanning imbibition curve  $p_{ci}[1]$  at saturation  $S_w[2]$  initiates a scanning drainage capillary pressure curve,  $p_{cd}[2]$ , back to  $S_w[1]$  to form a closed loop. At the two reversal points, the capillary pressures of the two scanning curves are equal,

$$p_{cd}[2](S_w[1]) = p_{ci}[1](S_w[1]), \quad (7)$$

$$p_{cd}[2](S_w[2]) = p_{ci}[1](S_w[2]). \quad (8)$$

The reversal at  $S_w[2]$  may occur for any saturation between  $S_w[1]$  and  $1-S_{or}[1]$ . The oil and water scanning curve asymptotes  $S_{or}[2]$  and  $S_{wr}[2]$  are the two unknowns in Eqs. 7 and 8, which are solved iteratively. A few iterations suffice.

**Third Reversal.** The  $p_{cd}[2]$ -process scans from  $S_w[2]$  back to  $S_w[1]$ . Any new reversal  $S_w[3]$ , before  $S_w[1]$  is reached, will scan back to  $S_w[2]$  again, i.e.,  $p_{ci}[3]$  is equal to  $p_{cd}[2]$  at  $S_w[3]$  and  $S_w[2]$ . If, however,  $S_w[1]$  is reached without any new reversal, the process shunted from a  $p_{cd}[2]$ -curve to a  $p_{cd}[0]$ -curve, i.e., it continues up the primary drainage curve.

**More Reversals.** Fig. 5 shows details of a set of enclosing scanning loops inside the bounding hysteresis loop. The first reversal (not shown) took place on the primary drainage curve  $p_{cd}[0]$  at the global residual water saturation  $S_{wr}$ , i.e., at  $S_w[1] = S_{wr}$ , initiating the bounding imbibition curve  $p_{ci}[1]$ , which in turn was reversed at  $S_w[2] = 1 - S_{or}$ , at the global residual oil saturation, and the secondary (bounding) drainage curve  $p_{cd}[2]$  was spawned. The scan from  $S_w[2]$  back to  $S_w[1]$  is now interrupted by the third reversal at  $S_w[3]$ , the first reversal point shown in the figure. The imbibition scan  $p_{ci}[3]$  from  $S_w[3]$  is aimed back at  $S_w[2]$ , but is interrupted at  $S_w[4]$  with a drainage process  $p_{cd}[4]$  that aims back at  $S_w[3]$ . Two more reversals occur, at  $S_w[5]$  and  $S_w[6]$ . From  $S_w[6]$  the drainage curve  $p_{cd}[6]$  scans to  $S_w[5]$ , and continue on the drainage process  $p_{cd}[4]$  to  $S_w[3]$ . Further drainage from  $S_w[3]$  follows the bounding drainage curve  $p_{cd}[2]$  back to  $S_{wr}$ , unless a new reversal occurs.

### Relative Permeability Functions.

We have developed a procedure similar to that of Corey and Burdine, reviewed in Ref. 27, to generate a relative permeability correlations for primary drainage and bounding imbibition and drainage curves for both oil and water, exemplified in Fig. 6. The development is based on Corey-type relative permeability functions which are inferred from the Brooks and Corey capillary pressure correlation for water-wet porous medium and the assumption of a bundle-of-tubes model for the pore network.

The general expression for capillary pressure, Eq. 2, consists of two Brooks-Corey type expressions, i.e., the water branch

$$p_{cw} = \frac{c_w}{\left( \frac{S_w - S_{wr}}{1 - S_{wr}} \right)^{a_w}}, \quad (9)$$

and the oil branch

$$p_{co} = \frac{c_o}{\left( \frac{S_o - S_{or}}{1 - S_{or}} \right)^{a_o}}. \quad (10)$$

Each of these branches may now be combined with a Corey-Burdine's integral over the capillary-tube size distribution<sup>27</sup> to render the wetting and non-wetting phase relative permeability functions. Note that the two branches in Eqs. 9 and 10 are for both drainage (index  $d$ ) and imbibition (index  $i$ ), four cases in all.

When performing the integral over the capillary tubes, with the water branch for drainage, i.e., with  $p_{c wd}$ , we get

$$k_{r wwd} = S_{nw}^{2a_{wd}+1+m_{wd}} \quad (11)$$

for the relative permeability to water, with water as the wetting phase, and

$$k_{r owd} = (1 - S_{nw}^{2a_{wd}+1})(1 - S_{nw})^{m_{od}} \quad (12)$$

for the oil relative permeability, with water as wetting phase.

If the same integration is performed with the oil branch  $p_{c od}$ , we get

$$k_{r wod} = (1 - S_{no}^{2a_{od}+1})(1 - S_{no})^{m_{wd}} \quad (13)$$

for drainage relative permeability to water in an oil-wet medium, and

$$k_{r ood} = S_{no}^{2a_{od}+1+m_{od}} \quad (14)$$

for relative permeability to oil in an oil-wet medium. Here  $m_{wd}$  and  $m_{od}$  are tortuosity exponents. Burdine<sup>3</sup> estimated a tortuosity exponent of 2.0 from experimental data. The normalized saturations are  $S_{nw} = (S_w - S_{wr}) / (1 - S_{wr} - S_{or})$  and  $S_{no} = (1 - S_w - S_{or}) / (1 - S_{wr} - S_{or})$ . For primary drainage,  $k_{r wwd}$  and  $k_{r owd}$  are used with  $S_{or} = 0$ , and similarly for primary imbibition.

**Normalized Saturations.** The normalized saturations,  $S_{nw}$  and  $S_{no}$ , in the Corey-type relative permeabilities are different from the normalized saturations in the capillary pressure correlation, Eq. 2. However, the  $a$ -values in the correlations are the same. If we multiply both the numerator and the denominator of the water branch term in Eq. 2 by

$$\left( \frac{1 - S_{wr}}{1 - S_{wr} - S_{or}} \right)^{a_w} \quad (15)$$

and the oil branch by

$$\left( \frac{1 - S_{or}}{1 - S_{wr} - S_{or}} \right)^{a_o}, \dots\dots\dots (16)$$

Eq. 2 becomes

$$p_c = \frac{c'_w}{\left( \frac{S_w - S_{wr}}{1 - S_{wr} - S_{or}} \right)^{a_w}} + \frac{c'_o}{\left( \frac{S_o - S_{or}}{1 - S_{or} - S_{wr}} \right)^{a_o}} \dots\dots (17)$$

with  $c_w$  redefined to  $c'_w$  by

$$c'_w = c_w \cdot \left( \frac{1 - S_{wr}}{1 - S_{wr} - S_{or}} \right)^{a_w} \dots\dots\dots (18)$$

and, correspondingly,

$$c'_o = c_o \cdot \left( \frac{1 - S_{or}}{1 - S_{wr} - S_{or}} \right)^{a_o} \dots\dots\dots (19)$$

**Tortuosity Exponent.** With all tortuosity exponents  $m$  equal to 2, as implied by Burdine, the Corey-type permeability expressions are strictly monotonic functions of saturation. They have no inflection point. Several researchers<sup>4,7,10,25,28-30</sup> have observed, however, inverted S-shape oil relative permeability curves with an inflection point, especially for the bounding oil imbibition curve.

Most of the measurements indicate that the bounding oil drainage curve lies below the bounding oil imbibition curve<sup>4,10,25,29-30</sup>. Illustrations by Honarpour<sup>31</sup> and measurements by Eikje,<sup>32</sup> however, indicate the opposite behavior. A general procedure therefore has to include both cases.

To allow for inverted S-shape curves, as well as being able to model cases with  $k_{roi} > k_{rod}$  and with  $k_{roi} < k_{rod}$ , we have introduced the tortuosity parameter  $m$  as a generalization of Burdine's<sup>3</sup> empirical tortuosity exponent of 2.0. Burdine introduced this factor to compensate for the fact that the porous medium is not a bundle of straight, non-interacting capillary tubes. We will use four tortuosity factors:  $m_{wd}$  and  $m_{od}$  for drainage, Eqs. 11–14,  $m_{wi}$  and  $m_{oi}$  for imbibition.

**Mixed Wettability.** The drainage relative permeability expressions, Eqs. 11–14, are for the limiting wettability states, i.e., completely oil-wet or completely water-wet. In a mixed-wet system, each phase moves partly as a wetting phase and partly as a non-wetting phase. It therefore seems reasonable that an expression valid for mixed wettability should be symmetric. That is, if parameters labeled by index  $w$  are swapped with parameters labeled by  $o$ , the functional form should be the same, e.g., the oil relative permeability function should look the same either the oil is considered to be the wetting or the non-wetting phase. Weighted summation of Eqs. 12 and 14 seems like a reasonable combination of the two limiting ex-

pressions, consistent with a concept of series coupling of fluid flow transmissibilities. The weighting should reflect the degree of wettability and it seems reasonable that a mixed-wettability curve should be between the two limiting curves, like in **Fig. 7** for the imbibition case.

**Weighting with  $p_c$ .** Earlier<sup>1</sup>, we proposed to weight the limiting relative permeability expressions by using the  $c$ -parameters in Eq. 2. This procedure implies constant wettability, independent of saturation. We do, however, suspect the wettability to be saturation dependent, to vary with pore radius and hence saturation. The thickness of the water film in the pores determines the degree of adsorption of surface active agents, which again affects the wettability.<sup>12</sup> The weight function should reflect continuous changes in wettability with saturation—a gradual change from water-wet conditions in the smaller pore channels to oil-wet behavior in the larger pores.

For example, an increase in water saturation from  $S_{wr}$  causes the water to invade small, water-wet pores and will reflect an associated change in relative permeability as for a water-wet system. At the other end, near  $S_{or}$ , the relative permeability curves should behave as for a completely oil-wet medium.

A saturation-dependent wettability is achieved by weighting the water-wet and oil-wet relative permeability functions, Eq. 11 and 13, with the respective water and oil branches of the capillary pressure function, Eq. 2, to give

$$k_{rwd} = k_{rw}^0 \cdot \frac{p_{cwd} k_{rwwd} - p_{cod} k_{rowd}}{p_{cwd} - p_{cod}} \dots\dots\dots (20)$$

for mixed-wet drainage relative permeability to water, where  $k_{rw}^0$  is the value of the bounding relative permeability curves at  $S_{or}$ , and

$$k_{rod} = k_{ro}^0 \cdot \frac{p_{cwd} k_{rowd} - p_{cod} k_{rowd}}{p_{cwd} - p_{cod}} \dots\dots\dots (21)$$

for relative permeability to oil, where  $k_{ro}^0$  is the value of the bounding relative permeability curves at  $S_{wr}$ . With index  $i$  substituting  $d$ , the equations are also valid for the imbibition process.

An example of the capillary pressure weight function for drainage,  $(p_{cwd} + p_{cod})/(p_{cwd} - p_{cod})$ , is shown in **Fig. 8**. It approaches completely water-wet conditions (+1 or ww) in the limit of  $S_{wr}$  and completely oil-wet conditions (-1 or ow) in the limit  $1 - S_{or}$ . There is one weight function for drainage and another for imbibition.

Primary drainage relative permeabilities may be modeled by  $k_{rwwd}$  and  $k_{ro}^0 \cdot k_{rowd}$ , with  $a_{wd}$  from a fit of the primary drainage capillary pressure, if such data are available. The default value of the tortuosity exponent  $m$  is the Burdine-value of 2.

**Matching Measured Data.** We have tested the relative permeability correlation on a consistent set of capillary pressure and relative permeability measurements published by Honarpour *et al.*<sup>10</sup>

In the expressions for relative permeability, Eqs. 20 and 21, the  $a$ -parameters of Eqs. 11–14, the  $c$ -parameters of the weight functions, and those for the imbibition case, all have the same values as in the corresponding capillary pressure correlation. The tortuosity exponents  $m$ , however, are optional parameters just for the relative permeability functions.

We obtain the  $a$ 's and  $c$ 's by curve-fitting the capillary pressure data, **Fig. 9**. Both types of parameters are subsequently employed in the mixed-wet relative permeability correlation. This implies that any change in the shape of the capillary pressure curve will be reflected in the relative permeability curves.

With the  $a$ 's and  $c$ 's from the capillary pressure correlation, and with all  $m$ 's equal to 2, we can make estimates of the relative permeability functions. They lie in the interval between 0 and 1 before estimates are made of the relative permeability endpoint values  $k_p^0$  of phase  $p$ .

The predictions are made in the same format as the measured data. If  $k_o(S_{wr})$  is chosen as reference value, then  $k_{ro}^0 = 1$ . As an estimate of  $k_{rw}^0$ , values from neighboring core plugs or from analogous porous media can be used. If no information is available, it seems reasonable to assume that the bounding imbibition relative permeability at  $S_{or}$  should be greater or equal to the primary drainage curve.<sup>33</sup> If no primary drainage data are known, an approximate value is  $k_{rwd}$  with  $a_{wd}$ . The estimate of  $k_{rw}^0$  then is  $k_{rwd}(S_{or})$ .

The first set of estimated relative permeability curves from the capillary pressure data can deviate considerably from the measured relative permeability data. Significant adjustments of the values of  $m$ ,  $k_{ro}^0$ , and  $k_{rw}^0$  may be needed. We used the Solver function of the Microsoft Excel spreadsheet to curve-fit relative permeability data by minimizing the sum of errors squared between the calculated and the measured relative permeability values. Each square error was multiplied by the  $k_r$ -value, but other weighting schemes might be preferable in other cases. The fit is shown in **Figs. 10–12**. In **Fig. 13** is shown the measured oil drainage data together with the fitted  $k_{rod}$ -curve and the limiting  $k_{rowd}$ - and  $k_{rood}$ -curves for oil- and water-wet systems, respectively.

Further evaluation of the  $p_c$ -weighting procedure should be done on consistent sets of capillary pressure and relative permeability data. Other weighting methods could also be tested.

### Relative Permeability Hysteresis Logic

Historically, relative permeability hysteresis has been considered of significance only between primary drainage and the imbibition curves. Many measurements have been made of these processes.<sup>7,26,28,34</sup> Hysteresis between secondary drainage and imbibition curves has also been recognized by several authors,<sup>4,10,25,29–30,32</sup> but there are few published data on relative permeability scanning curves. The most extensive set of measured scanning curves is that of Braun and Holland,<sup>4</sup> who used a pseudo-steady state method. A series of oil relative permeability scanning curves, originating on the bounding

imbibition and bounding drainage curve, were measured. These measurements show that

1. all oil drainage scanning curves originating on the bounding imbibition curve, **Fig. 14**, scan back towards  $S_{wr}$ ,  $k_{rw}^0$  and the bounding drainage curve,
2. all oil imbibition scanning curves spawned on the bounding drainage curve scan back towards  $k_{ro} = 0$  at  $S_{or}$ , approaching the bounding drainage curve, **Fig. 15**.

Both these observations are similar to those of Morrow<sup>21</sup> for the capillary pressure scanning curves.

The data<sup>4</sup> also show that the scanning loops are closed, i.e., a scanning curve from  $S_w[k]$  will scan back to  $S_w[k-1]$  and form a closed loop. Unless interrupted by another reversal, the process will proceed along the  $[k-2]$  curve, as if the  $[k-1]$  reversal had not occurred. This is demonstrated in **Figs. 16–17**.

Braun and Holland<sup>4</sup> find the relative permeability scanning curves to be reversible. However, the saturation intervals of the scanning loops are so small that hysteresis, if present, would experimentally be difficult to detect, e.g., the modeled results in **Figs. 16–17** which are closely resembling some of the measured cases.

Also, we will expect that both water and oil relative permeability in a mixed-wet system will exhibit similar hysteretic behavior and that oil relative permeability in a water-wet system will exhibit negligible hysteresis, as does water relative permeability in a water-wet system.

**Procedure.** The suggested procedure for modeling relative permeability scanning curves is consistent and integrated with the procedure for modeling of the capillary pressure scanning curves. The same convention for labels is used: all properties of the  $k$ 'th scanning curve are labeled by  $[k]$ . The relative permeability functions are denoted by  $k_{rod}[k]$ ,  $k_{rwd}[k]$ ,  $k_{roi}[k]$ , and  $k_{rwi}[k]$ , and saturation reversals occur at  $S_w[k]$ . For imbibition curves, defined by increasing water saturation, all labels have odd numbers while they are even for drainage curves. Hence, the first imbibition relative permeability curves from primary drainage are denoted  $k_{roi}[1]$  and  $k_{rwi}[1]$ . We make an exception from this convention for the 'bounding (secondary) drainage curve' which returns the process from  $S_{or}[1]$ , back to  $S_w[1]$ . This drainage process will have associated functions  $p_{cd}[1]$ ,  $k_{rod}[1]$  and  $k_{rwd}[1]$ . For the special case if  $S_w[2] = 1 - S_{or}[1]$ , then  $p_{cd}[2] = p_{cd}[1]$ , and similarly for  $k_{rod}[2]$  and  $k_{rwd}[2]$ .

The limiting relative permeability expressions, i.e., the expressions for completely water- and oil-wet systems, are functions of the normalized saturations  $S_{no}$  and  $S_{nw}$ . They are now generalized to

$$S_{nw} = \frac{S_w - S_{wr}}{1 - S_{wr} - S_{or}[1]} \dots\dots\dots(22)$$

and

$$S_{no} = \frac{S_o - S_{or}[1]}{1 - S_{wr} - S_{or}[1]} \quad (23)$$

If the first reversal from the primary drainage curve occurs at irreducible water saturation, i.e.,  $S_w[1] = S_{wr}$ , then  $S_{or}[1] = S_{or}$  and  $S_{nw}$  and  $S_{no}$  revert to their previous definitions.

We also need to generalize the weighting procedure for cases when the water saturations exceeds  $1 - S_{or}$ , which may occur if  $S_w[1] > S_{wr}$ . Instead of the weight  $p_{coi}$ , the imbibition oil branch of Eq. 2, we use  $p_{cod}$  instead of  $p_{cod}[1]$ , and no changes in the water-branch weight. This general weighting procedure approaches the previously defined procedure with the bounding capillary pressure branches, Eqs. 20–21, when  $S_w[1]$  approaches  $S_{wr}$ . In this manner, if  $S_w[1] > S_{wr}$ , the scanning curves will be mixed-wet near  $S_w[1]$  and completely oil-wet at  $S_{or}[1]$ , which seems reasonable. If we assume that primary drainage occurs at water-wet conditions, the porous medium will be subject to aging before any reversal occurs. It is therefore perhaps reasonable with an initial discontinuity in wettability.

With the general definition of the weighting procedure and the normalized saturations, the relative permeability functions are defined between the global residual saturations  $S_{wr}$  and  $S_{or}[1]$ . The scanning curves are to defined in the interval between  $S_w[k]$  and  $S_w[k-1]$ , or as a special case, between  $S_w[1]$  and  $1 - S_{or}[1]$ .

We introduce an additional parameter,  $k_{tpa}[k]$ , representing a fictitious threshold relative permeability value—the scanning relative permeability value at the global residual saturation of the phase in question. **Fig. 18** illustrates the  $k_{rod}[k]$ -value for a drainage reversal from an imbibition curve. There are four  $k_{tpa}[k]$ -values, one for each combination of phase  $p$  and process **a**. We may then formulate the following general expressions for mixed-wet, scanning, relative permeability functions,

$$k_{rwd}[k] = k_{rwd}^0 \frac{p_{cwd}k_{rwd} - p_{cod}[1]k_{rowd}}{p_{cwd} - p_{cod}[1]} + k_{rwd}^t[k], \quad (24)$$

$$k_{rod}[k] = k_{rod}^0 \frac{p_{cwd}k_{rowd} - p_{cod}[1]k_{rood}}{p_{cwd} - p_{cod}[1]} + k_{rod}^t[k], \quad (25)$$

$$k_{rwi}[k] = k_{rwi}^0 \frac{p_{cwi}k_{rwwi} - p_{coi}[1]k_{rowi}}{p_{cwi} - p_{coi}[1]} + k_{rwi}^t[k], \quad (26)$$

and

$$k_{roi}[k] = k_{roi}^0 \frac{p_{cwi}k_{rowi} - p_{coi}[1]k_{rooi}}{p_{cwi} - p_{coi}[1]} + k_{roi}^t[k], \quad (27)$$

where  $k_{tpa}^0[k]$  is a scaling parameter that represents the absolute difference between the function values  $k_{tpa}[k](S_{wr})$  and  $k_{tpa}[k](S_{or}[1])$ . Eqs. 24–27 revert to the bounding imbibition and drainage curves in the limit when  $S_w[1] = S_{wr}$ , Eqs. 20–21, and may be written in the compact form,

$$k_{rwd}[k](S_w) = k_{rwd}^0[k] \cdot k_{rwd}[1](S_w) + k_{rwd}^t[k], \quad (28)$$

$$k_{rod}[k](S_w) = k_{rod}^0[k] \cdot k_{rod}[1](S_w) + k_{rod}^t[k], \quad (29)$$

$$k_{rwi}[k](S_w) = k_{rwi}^0[k] \cdot k_{rwi}[1](S_w) + k_{rwi}^t[k], \quad (30)$$

$$k_{roi}[k](S_w) = k_{roi}^0[k] \cdot k_{roi}[1](S_w) + k_{roi}^t[k]. \quad (31)$$

Each expression has two adjustable parameters,  $k_{tpa}^0[k]$  and  $k_{tpa}^t[k]$ . The two equations needed are found by enforcing closed scanning loops, i.e., that the two scanning curves give the same relative permeability value at the start and end of the loop.

**First Reversal.** A first saturation reversal at  $S_w[1]$  on the primary drainage curve spawns an imbibition process, labeled [1] which scans towards  $S_{or}[1]$ , **Figs. 19–20**. For the case when  $S_w[1] = S_{wr}$ , the imbibition curve is the bounding imbibition curve and  $S_{or}[1]$  is equal to  $S_{or}$ . Consistent with the hysteresis logic for the capillary pressure curves,  $S_{or}[1]$  is determined by Land's<sup>34</sup> trapping relation, Eq. 6.

**Oil Relative Permeability.** The imbibition oil relative permeability curve scans from

$$k_{roi}[1](S_w[1]) = k_{rod}[0](S_w[1]) \quad (32)$$

at the reversal point to

$$k_{roi}[1](S_{or}[1]) = 0 \quad (33)$$

at the residual oil saturation. Since the curve is ‘anchored’ with  $k_{roi} = 0$ , also  $k_{roi}^t[1] = 0$ . Eq. 32 is therefore solved with respect to  $k_{roi}^0[1]$ .

**Water Relative Permeability.** The water relative permeability curve scans from the reversal point on the primary drainage curve, which requires that

$$k_{rwi}[1](S_w[1]) = k_{rwd}[0](S_w[1]), \quad (34)$$

which corresponds to Eq. 32. At the other endpoint  $S_{or}[1]$ ,

$$k_{rwi}[1](S_{or}[1]) = k_{rw}^0(S_{or}[1]), \quad (35)$$

where  $k_{rw}^0$  is a certain function of the residual oil saturation, see e.g., discussion in Standing's report.<sup>2</sup> To our knowledge, no study has been published on this relation. We have therefore chosen to use linear interpolation between  $k_{rwi}(S_{or})$ , endpoint for bounding imbibition curve, and  $k_{rwd}[0](S_w=1) = 1$  to determine  $k_{rw}^0(S_{or}[1])$ . The same method is used by Killough<sup>14</sup> and Eikje *et al.*<sup>32</sup>

**Second Reversal.** A second reversal will start a drainage process, labeled [2], from the reversal saturation  $S_w[2]$ , aiming back at  $S_w[1]$ .

**Oil Relative Permeability.** The oil relative permeability curve scans from

$$k_{rod}[2](S_w[2]) = k_{roi}[1](S_w[2]) \quad \dots\dots\dots (36)$$

at the new reversal point, to

$$k_{rod}[2](S_w[1]) = k_{roi}[1](S_w[1]) \quad \dots\dots\dots (37)$$

at the previous reversal point [1], in this case on the primary drainage curve. The  $k_{rod}[2]$ -curve is shown in **Fig. 19**.

**Water Relative Permeability.** Equations for the water relative permeability scanning curve are

$$k_{rwd}[2](S_w[2]) = k_{rwi}[1](S_w[2]) \quad \dots\dots\dots (38)$$

and

$$k_{rwd}[2](S_w[1]) = k_{rwi}[1](S_w[1]), \quad \dots\dots\dots (39)$$

and the  $k_{rwd}[2]$ -curve is shown in **Fig. 20**.

The drainage process [2] will scan back to reversal point [1] and subsequently follow the primary drainage curve, labeled [0]. Any new reversal will thereafter be equivalent to a first reversal. A third reversal may, however, occur before the process reaches back to reversal point [1].

**Third Reversal.** A third reversal before the process reaches back to [1] will start an imbibition process from saturation reversal  $S_w[3]$ , scanning back to  $S_w[2]$ . If this process, labeled [3], passes through reversal point [2], it will retrace process [1].

**Oil Relative Permeability.** The third oil imbibition relative permeability curve scans from

$$k_{roi}[3](S_w[3]) = k_{rod}[2](S_w[3]) \quad \dots\dots\dots (40)$$

at the new reversal point, to

$$k_{roi}[3](S_w[2]) = k_{rod}[2](S_w[2]) \quad \dots\dots\dots (41)$$

at the previous reversal point.

**Water Relative Permeability.** The equations for the water relative permeability scanning curve are

$$k_{rwi}[3](S_w[3]) = k_{rwd}[2](S_w[3]) \quad \dots\dots\dots (42)$$

and

$$k_{rwi}[3](S_w[2]) = k_{rwd}[2](S_w[2]) \quad \dots\dots\dots (43)$$

**General Reversals.** The methodology for creating scanning curves may easily be generalized from the observations that they form closed loops, i.e., a process with reversal at  $S_w[k]$  will return to  $S_w[k-1]$ .

**Figs. 21–22** show one closed scanning loop  $[k]-[k+1]-[k]$ , inside of an outer scanning loop  $[k-2]-[k-1]-[k-2]$ . The outer loop has an imbibition process from  $[k-2]$  to  $[k-1]$ , where the saturation change is reversed. The drainage curve scans back to  $[k-2]$  but is interrupted by the inner loop's imbibition process from  $[k]$  to  $[k-1]$ . This process is interrupted at  $[k+1]$ , with a drainage scan back to  $[k]$ . Continued drainage after reaching

$[k]$  causes tracing of the drainage scanning curve from  $[k-1]$  to  $[k-2]$ .

**Imbibition Oil Relative Permeability.** The general oil imbibition relative permeability curve scans from

$$k_{roi}[k](S_w[k]) = k_{rod}[k-1](S_w[k]) \quad \dots\dots\dots (44)$$

at reversal point  $[k]$  to

$$k_{roi}[k](S_w[k-1]) = k_{rod}[k-1](S_w[k-1]) \quad \dots\dots\dots (45)$$

at reversal point  $[k-1]$ .

The two unknown parameters  $k_{roi}^0[k]$  and  $k_{roi}^t[k]$  of imbibition scanning curve labeled  $[k]$  may be expressed by

$$k_{roi}^0[k] = k_{rod}^0[k-1] \times \left\{ \frac{k_{rod}[1](S_w[k]) - k_{rod}[1](S_w[k-1])}{k_{roi}[1](S_w[k]) - k_{roi}[1](S_w[k-1])} \right\}, \quad \dots\dots\dots (46)$$

and

$$k_{roi}^t[k] = k_{rod}^t[k-1] + k_{rod}^0[k-1] \cdot k_{rod}[1](S_w[k]) - k_{roi}^0[k] \cdot k_{roi}[1](S_w[k]), \quad \dots\dots\dots (47)$$

when Eqs. 29 and 31 are introduced in Eqs. 44–45.

**Imbibition Water Relative Permeability.** Quite similarly the general equations for water relative permeability curves can be formulated as

$$k_{rwi}[k](S_w[k]) = k_{rwd}[k-1](S_w[k]) \quad \dots\dots\dots (48)$$

at reversal point  $[k]$  to

$$k_{rwi}[k](S_w[k-1]) = k_{rwd}[k-1](S_w[k-1]) \quad \dots\dots\dots (49)$$

at reversal point  $[k-1]$ , and

$$k_{rwi}^0[k] = k_{rwd}^0[k-1] \times \left\{ \frac{k_{rwd}[1](S_w[k]) - k_{rwd}[1](S_w[k-1])}{k_{rwi}[1](S_w[k]) - k_{rwi}[1](S_w[k-1])} \right\}, \quad \dots\dots\dots (50)$$

and

$$k_{rwi}^t[k] = k_{rwd}^t[k-1] + k_{rwd}^0[k-1] \cdot k_{rwd}[1](S_w[k]) - k_{rwi}^0[k] \cdot k_{rwi}[1](S_w[k]), \quad \dots\dots\dots (51)$$

If the  $i$ 's and  $d$ 's are swapped, the equations are equally valid for general drainage scanning curves.

This hysteresis logic is general and few modifications are needed if another relative permeability model or weighting procedure is chosen.

## Discussion

**Validation of Hysteresis Logic.** The hysteresis model has not yet been quantitatively checked against measured data. It has been designed, however, to qualitatively honor the characteristic features of the measurements of Braun and Holland,<sup>4</sup> who did not measure capillary pressure.

The lack of consistent capillary pressure and relative permeability measurements on the same core sample makes it difficult to determine the  $a$ 's and  $c$ 's for the capillary pressure correlation. A series of measurements for checking the model should encompass the capillary pressure and relative permeability of the bounding hysteresis loop and a variety of scanning curves and loops, possibly measured by a technique similar to that of Honarpour *et al.*<sup>10</sup>

**Figs. 16–17** show that modeled scanning loops exhibit negligible hysteresis when  $\Delta S_w = S_w[k] - S_w[k-1]$  is small, in accordance with the observations of Braun and Holland.<sup>4</sup> Furthermore, modeled scanning curves originating on the bounding imbibition or drainage curve all scan back to the residual phase saturation, **Figs. 14–15**. This is also in agreement with the observations by Braun and Holland.

No attempt has been made to model the measured scanning curves of Braun and Holland<sup>4</sup> with capillary pressure parameters  $a$  and  $c$  determined from matching their measured bounding *relative permeability* curves. This would probably not give any definite arguments to keep or reject the model. As discussed in detail by Lohne,<sup>35</sup> the starting points of the scanning curves, i.e., the saturation reversal points of Braun and Holland, are not properly located on the bounding hysteresis loop, which was measured first.

**Scaling.** Kriebenegg and Heinemann<sup>36</sup> chose to scale the whole bounding drainage and imbibition curves to model the scanning curves. We believe that scaling of just a section of the  $k_{rpa}[1]$ -curve is more reasonable. Then, if there is no hysteresis between the bounding imbibition and drainage curves, a drainage scanning curve from the bounding imbibition curve will exhibit no hysteresis, regardless of size of the saturation interval ( $S_w[k] - S_{wr}$ ). If scaling of the whole bounding drainage curve between  $S_w[k]$  and  $S_{wr}$  is chosen, however, the hysteresis become more pronounced as the range of the interval decreases.

## Conclusions

1. A new two-phase model for mixed-wet relative permeability curves is developed and covers primary drainage, imbibition, and secondary drainage. The correlation is the sum of two Corey-type relative permeability expressions, weighted with the branches of the capillary pressure correlation.
2. The two Corey expressions represent completely water- and oil-wet systems. Through the weighting, the wettability is made saturation dependent.
3. The relative permeability correlation is integrated and bundled with the capillary pressure correlation.
4. In addition to the capillary pressure, an extra set of pa-

rameters are introduced to improve the match of relative permeability data, e.g., tortuosity factors.

5. Curve-fitting a consistent set of capillary pressure and relative permeability data gives good results.
6. An associated hysteresis logic treats scanning curves from primary drainage and inside the bounding hysteresis loop. Modeled hysteresis curves exhibit the same behavior as observed by Braun and Holland.
7. The hysteresis logic is a unified procedure for relative permeability and capillary pressure functions.
8. Further validation should be made from consistent and simultaneously measured datasets of capillary pressure and relative permeability scanning curves.
9. A systematic study of tortuosity factors and endpoint values of relative permeability is needed.

## Nomenclature

- $a$  = constant, dimensionless
- $c$  = constant, psi, bar or mbar
- $k$  = saturation reversal counter
- $k_r$  = relative permeability, dimensionless
- $m$  = tortuosity exponent, dimensionless
- $p$  = pressure, psi, bar or mbar
- $C$  = Land's trapping constant, dimensionless
- $S$  = saturation
- $[k]$  = label, saturation reversal number  $k$  and the subsequent scanning curve

## Subscripts

- $c$  = capillary
- $d$  = drainage
- $i$  = imbibition or initial
- $n$  = normalized
- $o$  = oil or oil-wet
- $p$  = phase ( $o$  or  $w$ )
- $r$  = residual or relative
- $w$  = water or water-wet
- $a$  = process ( $d$  for drainage or  $i$  for imbibition)
- $0$  = zero point ( $p_c = 0$ )

## Superscripts

- $t$  = threshold
- $0$  = endpoint

## Acknowledgements

We thank E.M. Braun and M.M. Honarpour for giving us access to unique relative permeability data, and to J. A. Larsen for constructive assistance. We would also like to thank Den norske stats oljeselskap a.s. (Statoil) for support and permission to publish the paper.

## References

1. Skjæveland, S.M., Siqveland, L.M., Kjosavik, A., Hammervold, W.L., and Virmovsky, G.A.: "Capillary Pressure Correlation for Mixed-Wet Reservoirs," paper SPE 39497 presented at the 1998 SPE India Oil and Gas Conference, NewDelhi, India, April, 7–9.



2. Standing, M.B.: "Notes on Relative Permeability Relationships," *Proc.*, U. of Trondheim, NTH, Norway (1975).
3. Burdine, N.T.: "Relative Permeability Calculations From Pore Size Distribution Data," *Trans. AIME* (1953) **198**, 71–77.
4. Braun, E.M. and Holland, R.F.: "Relative Permeability Hysteresis: Laboratory Measurements and a Conceptual Model," *SPERE* (Aug. 1995) 222–28.
5. Huang, D.D., Honarpour, M.M., and Al-Hussainy, R.: "An Improved Model for Relative Permeability and Capillary Pressure Incorporating Wettability," paper presented at the 1997 Society of Core Analysts International Symposium, Calgary, Sept. 7–10.
6. Lenhard, R.J. and Oostrom M.: "A Parametric Model for Predicting Relative Permeability-Saturation-Capillary Pressure Relationships of Oil-Water Systems in Porous Media with Mixed Wettability," *Transport in Porous Media* (1998) **31**, 109–131.
7. Osoba, J.S., Richardson, J.G., Kerver, J.K., Hafford, J.A., and Blair, P.M.: "Laboratory Measurements of Relative Permeability," *Trans. AIME* (1956) **192**, 47–56.
8. Hagoort, J.: "Measurements of relative permeability for computer modeling/reservoir simulation," *Oil & Gas Journal* (Feb. 1984) 62–68.
9. Chierici, G.L.: "Novel Relations for Drainage and Imbibition Relative Permeabilities," paper SPE 10165 presented at the 1981 SPE Annual Technical Conference and Exhibition, San Antonio, Texas, Oct. 5–7.
10. Honarpour, M.M., Huang, D.D., and Al-Hussainy, R.: "Simultaneous Measurements of Relative Permeability, Capillary Pressure, and Electrical Resistivity with Microwave System for Saturation Monitoring," *SPE Journal* (Sep. 1996) 283–295.
11. McDougall, S.R. and Sorbie, K.S.: "The Impact of Wettability on Waterflooding: Pore-Scale Simulation," *SPERE* (Aug. 1995) 208–213.
12. Anderson, W.G.: "Wettability Literature Survey – Part 5: Effect of Wettability on Relative Permeability," *JPT* (Nov. 1987) 1453–1468.
13. Guzmán, R.E. and Fayers, F.J.: "Mathematical Properties of Three-Phase Flow Equations," *SPE Journal* (Sep. 1997) 291–300.
14. Killough, J.E.: "Reservoir Simulation With History-Dependent Saturation Functions," *SPEJ* (Feb. 1976) 37–48, *Trans.*, AIME, **261**.
15. Laroche, C., Vizika, O., and Kalaydjian, F.: "Network Modeling to Predict the Effect of Wettability Heterogeneities on Multi-phase Flow," paper SPE 56674 presented at the 1999 SPE Annual Technical Conference and Exhibition, Houston, Texas, Oct. 3–6.
16. Larsen, J.A. and Skauge, A.: "Simulation of the Immiscible WAG Process Using Cycle-Dependent Three-Phase Relative Permeabilities," paper SPE 56475 presented at the 1999 SPE Annual Technical Conference and Exhibition, Houston, Texas, Oct. 3–6.
17. Moulou, J.-C., Vizika, O., Egermann, P., and Kalaydjian, F.: "A New Three-Phase Relative Permeability Model For Various Wettability Conditions," paper SPE 56477 presented at the 1999 SPE Annual Technical Conference and Exhibition, Houston, Texas, Oct. 3–6.
18. Alpak, F.O., Lake, L.W., and Embid, S.M.: "Validation of a Modified Carman-Kozeny Equation To Model Two-Phase Relative Permeabilities," paper SPE 56479 presented at the 1999 SPE Annual Technical Conference and Exhibition, Houston, Texas, Oct. 3–6.
19. Brooks, R.H. and Corey, A.T.: "Hydraulic Properties of Porous Media," Hydraulic Paper No. 3, Colorado State University, 1964.
20. Brooks, R.H. and Corey, A.T.: "Properties of Porous Media Affecting Fluid Flow," *J. of the Irrigation and Drainage Division, Proc. of ASCE*, **92**, No. IR2, (1966) 61–88.
21. Morrow, R. and Harris, C.C.: "Capillary Equilibrium in Porous Media," *SPEJ* (March 1965) 15–24.
22. Wardlaw, N.C. and Taylor, R.P.: "Mercury Capillary Pressure Curves and the Interpretation of Pore Structure and Capillary Behaviour in Reservoir Rocks," *Bull. Can. Pet. Geo.*, **24**, No. 2 (June 1976) 225–62.
23. Hammervold, W.L., Knutsen, Ø., Iversen, J.E., and Skjæveland, S.M.: "Capillary Pressure Scanning Curves by the Micropore Membrane Technique," *J. Pet. Sci. & Eng.* (1998) **20**, 253–258.
24. Topp, G.C. and Miller, E.E.: "Hysteretic Moisture Characteristics and Hydraulic Conductivities for Glass-Bead Media," *Soil Sci. Soc. Amer. Proc.* (1966) **30**, 156–162.
25. Colonna, J., Brissaud, F., and Millet, J.L.: "Evolution of Capillarity and Relative Permeability Hysteresis," *SPEJ* (Feb. 1972) 28–38; *Trans.*, AIME, **253**.
26. Land, C.S.: "Calculation of Imbibition Relative Permeability for Two- and Three Phase Flow From Rock Properties," *SPEJ* (June 1968) 149–56; *Trans.*, AIME, **243**.
27. Amyx, J.W., Bass, D.M., and Whiting, R.T.: *Petroleum Reservoir Engineering*, McGraw-Hill, New York (1960) 133–210.
28. Geffen, T.M., Owens, W.W., Parrish, D.R., and Morse, R.A.: "Experimental Investigation of Factors Affecting Laboratory Relative Permeability Measurements," (1951) 99–110, *Trans.*, AIME, **192**.
29. Evrenos, A.I. and Comer, A.G.: "Numerical Simulation of Hysteretic Flow in Porous Media," paper SPE 2693 presented at the 1969 SPE Annual Fall Meeting, Denver, Colorado, Sept. 28–Oct. 1.
30. Braun, E.M.: "A Steady-State Technique for Measuring Oil-Water Relative Permeability Curves at Reservoir Conditions," paper SPE 10155 presented at the 1981 SPE Annual Technical Conference and Exhibition, San Antonio, Texas, Oct. 5–7.
31. Honarpour, M., Koederitz, L., and Harvey, A.H.: *Relative Permeability of Petroleum Reservoirs*, CRC Press, Inc. (1986).
32. Eikje, E., Jakobsen, S.R., Lohne, A., and Skjæveland, S.M.: "Relative Permeability Hysteresis in Micellar Flooding," *J. Pet. Sci. Eng.* (1992) **7**, No. 1–2, 91–103.
33. Larsen, J.A.: "Evaluation of Transport Properties for Immiscible Flow in Porous Media," PhD dissertation, U. Bergen, Bergen, Norway (1997).
34. Land, C.S.: "Comparison of Calculated with Experimental Imbibition Relative Permeability," *SPEJ* (Dec. 1971) 419–425, *Trans.*, AIME, **251**.
35. Lohne, A.: "Hysteresis in Two- and Three-Phase Flow in Porous Medium," MS thesis, Stavanger College, Stavanger, Norway (1998).
36. Kriebner, M. and Heinemann, Z.: "A New Model for History Dependent Saturation Functions in Reservoir Simulation," paper presented at the 1996 European Conference on the Mathematics of Oil Recovery, Leoben, Austria, Sept. 3–6.

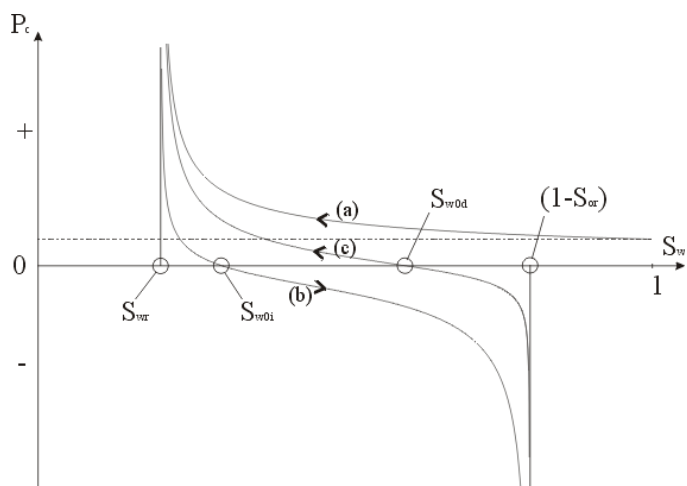


Fig. 1—Capillary pressure curves for (a) primary drainage, (b) bounding imbibition and (c) secondary drainage.

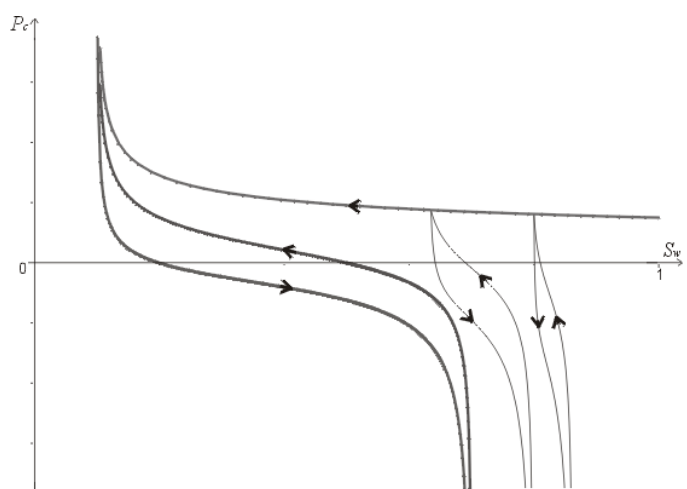


Fig. 2—Capillary pressure scanning curves originating on the primary drainage curve.

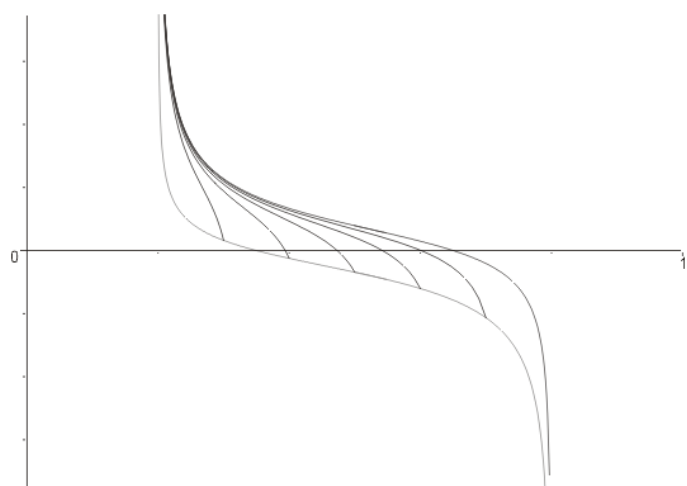


Fig. 3—Drainage capillary pressure scanning curves originating on the bounding imbibition curve.

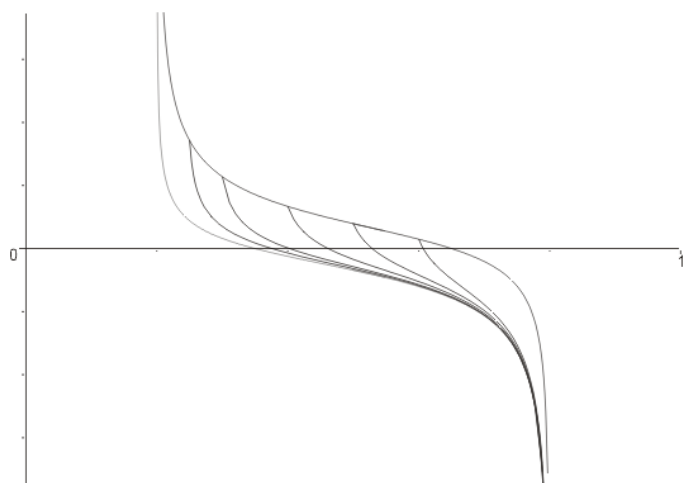


Fig. 4—Imbibition capillary pressure scanning curves originating on the bounding drainage curve.

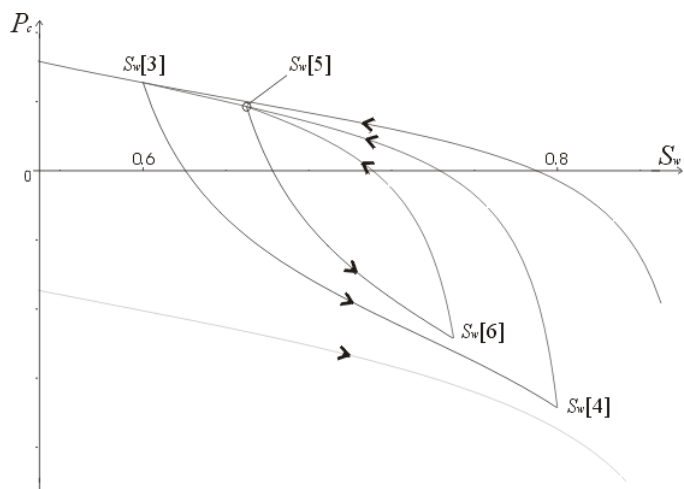


Fig. 5—Closed capillary pressure scanning loops.

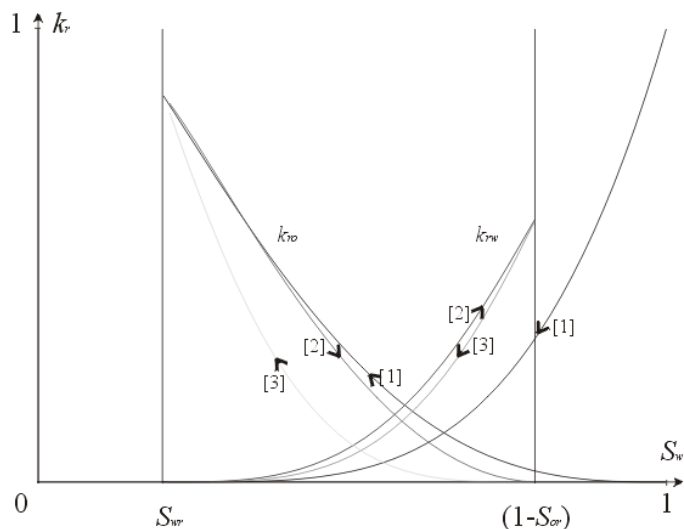


Fig. 6—Relative permeability curves for [1] primary drainage, [2] bounding imbibition and [3] secondary (bounding) drainage.

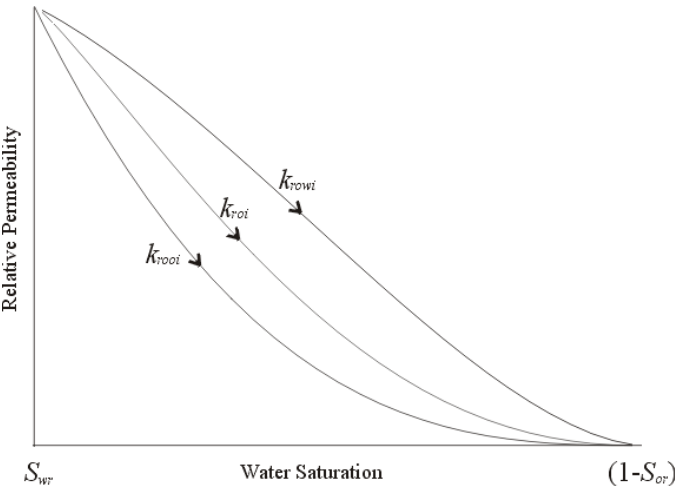


Fig. 7—Limiting oil imbibition relative permeability curves (cf. Eqs. 12 and 14 for the drainage case) and resulting mixed-wet relative permeability  $k_{roi}$ .

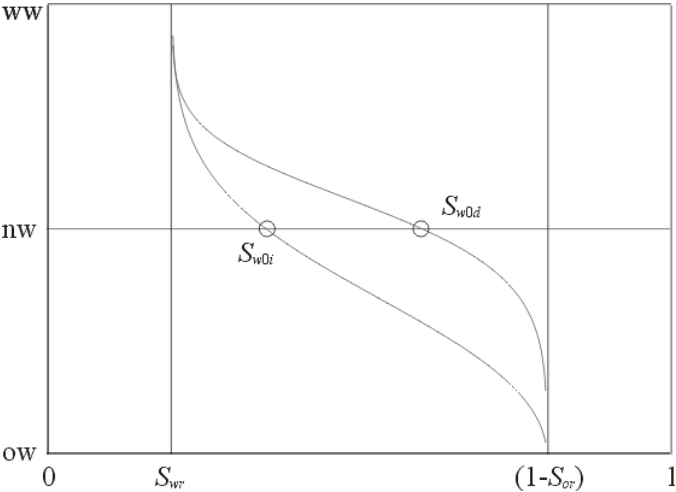


Fig. 8—Example of capillary pressure weight functions; ww: water-wet; nw: neutral-wet; ow: oil-wet.

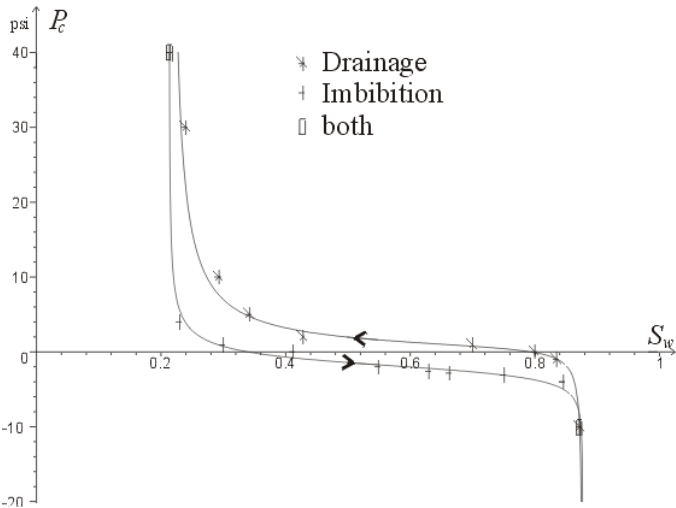


Fig. 9—Capillary pressure correlation fitted to data measured by Honarpour *et al.*<sup>10</sup>

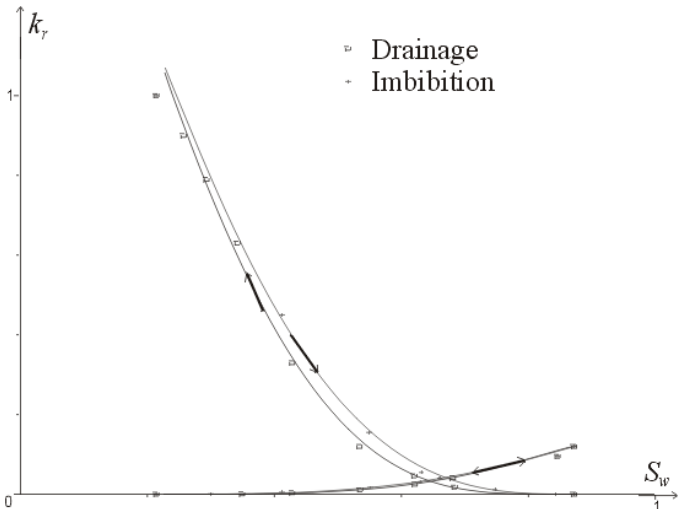


Fig. 10—Relative permeability correlation fitted to measured data by Honarpour *et al.*<sup>10</sup>

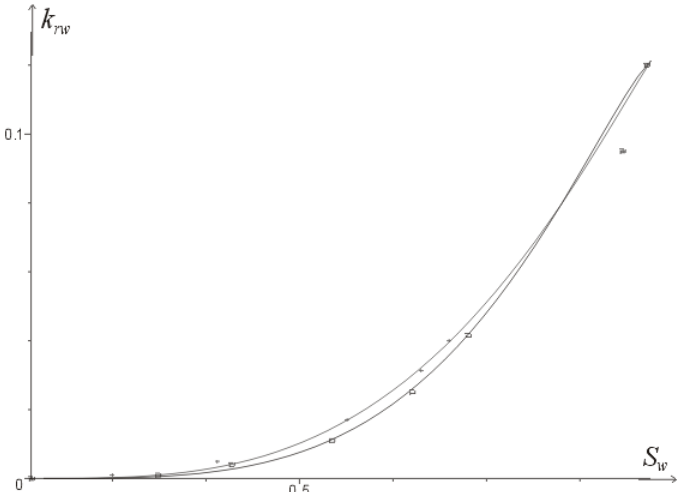


Fig. 11—Detail of Fig. 10, water relative permeability.

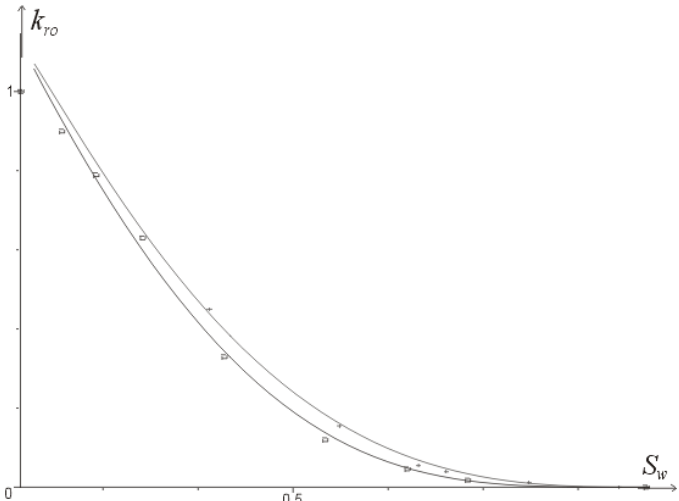


Fig. 12—Detail of Fig. 10, oil relative permeability.

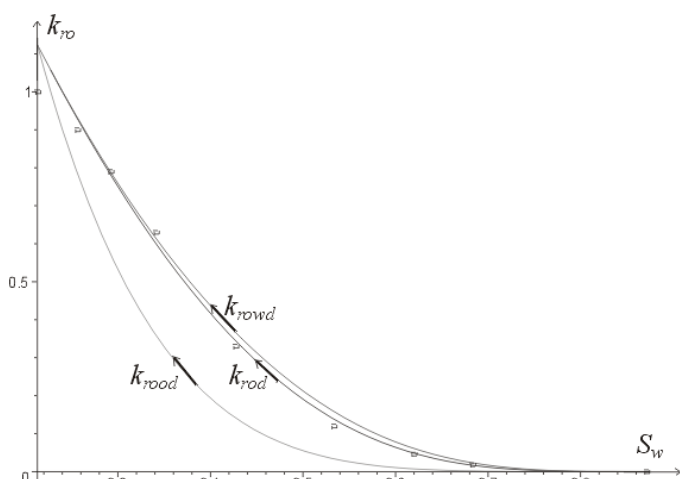


Fig. 13—Limiting and predicted drainage oil relative permeability curves, together with measured data.



Fig. 14—Oil drainage scanning curves originating on the bounding imbibition curve.

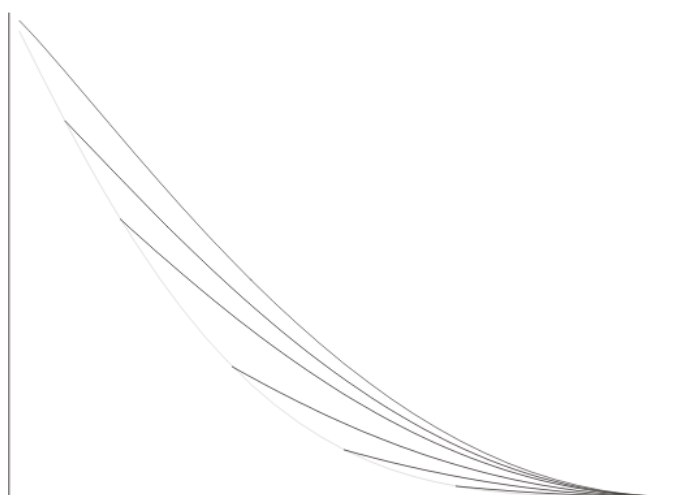


Fig. 15—Oil imbibition scanning curves originating on the bounding drainage curve.

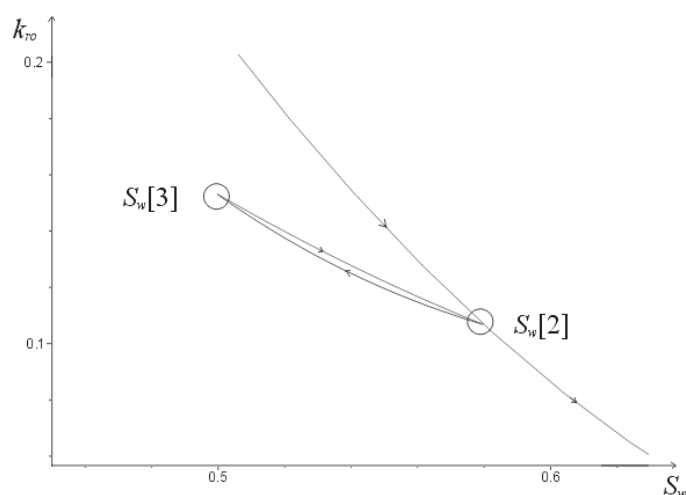


Fig. 16—Modeled closed scanning loop originating on bounding imbibition curve.

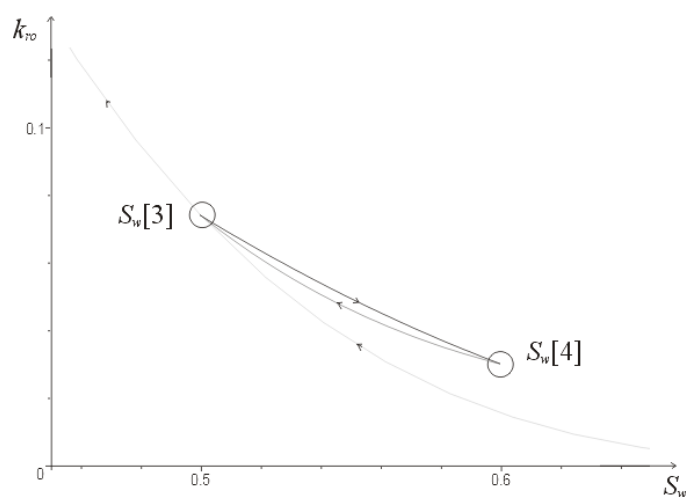


Fig. 17—Modeled closed scanning loop originating on the bounding drainage curve.

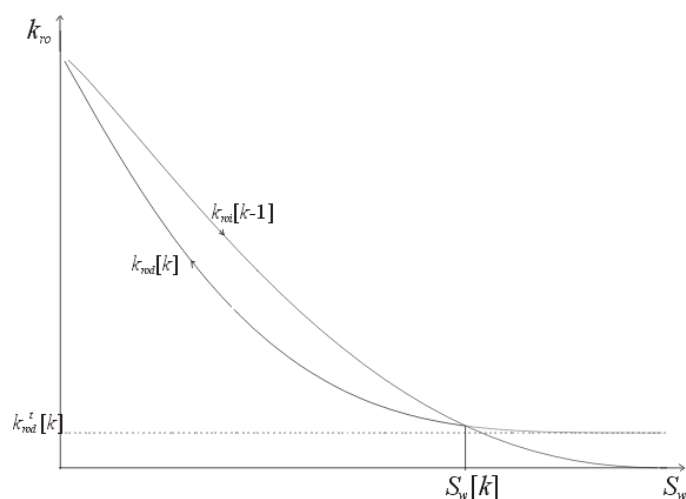


Fig. 18—Drainage scanning curve originating on bounding imbibition curve. Horizontal line represents the value of  $k_{rod}^t[k]$ .

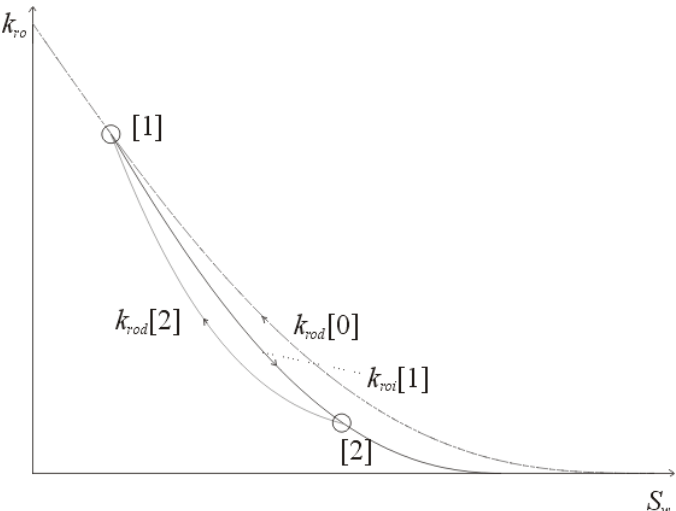


Fig. 19—Oil relative permeability scanning curves originating from reversal [1] on the primary drainage curve,  $k_{rod}[0]$ .

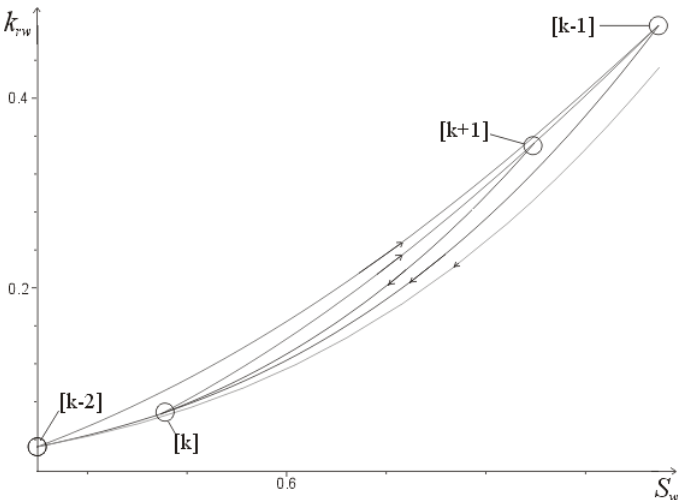


Fig. 22—Modeled scanning loops for water relative permeability.

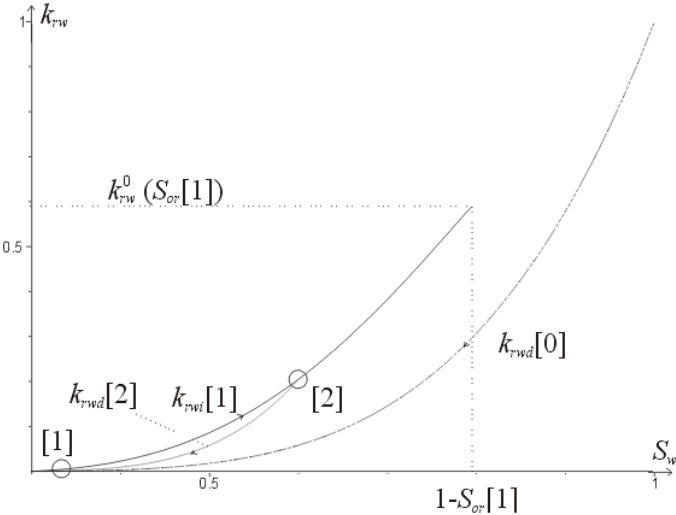


Fig. 20—Water relative permeability scanning curves originating from reversal [1] on the primary drainage curve  $k_{rwd}[0]$ .

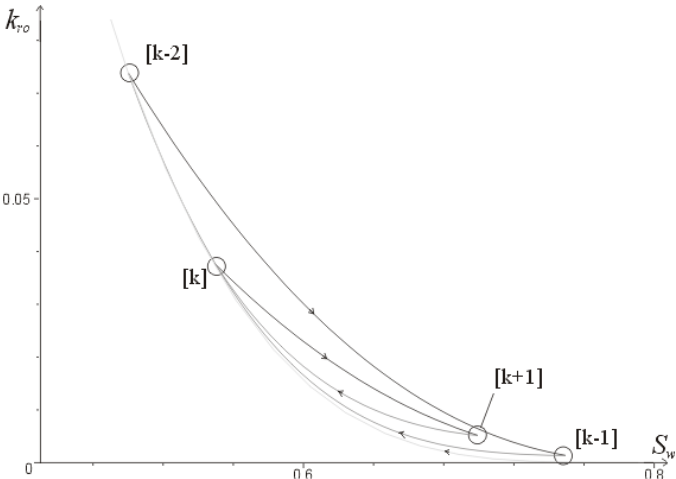


Fig. 21—Modeled scanning loops for oil relative permeability.